

One Step Synthesis and Optical Evaluation of Copper Oxide (CuO) Nanoparticles

*M. Abdul Momin¹, Roksana Pervin¹, M. Jalal Uddin¹
G.M. Arifuzzaman Khan² and Momtazul Islam¹

¹Dept of Applied Physics, Electronics and Communication Engineering,
Islamic University, Kushtia, Bangladesh

²Department of Applied Chemistry and Chemical Technology, Islamic University, Kushtia, Bangladesh

Abstract

One-dimensional nanostructural materials are currently the focus of considerable interest. Many methods have been used for the preparation of nanoparticles. However, to our knowledge, complex process control, high reaction temperatures or long synthesis time may be required for these approaches. Here we report a novel and simple one-step for synthesis of highly stable and freestanding cupric oxide (CuO) nanoparticles of approximately 10 and 12 nm in size which have been successfully synthesized via electrochemical method. Ultraviolet-visible spectroscopy (UV-VIS), X-ray diffraction (XRD) and Fourier transformation infrared spectroscopy (FTIR) were introduced to characterize the samples. The results indicate that growth conditions are responsible for different sizes.

1. Introduction

Nanoscale quantum dots have been extensively studied in order to understand the evolving electronic structure from atomic to bulk state. The properties of nanoclusters cannot be described simply as a straightforward extension of molecules or bulk solids. Understanding the fundamental properties of quantum dots rely on the ability to synthesize nanocrystals having a narrow size distribution with well controlled surfaces and defects. Investigations on size dependent electronic structure [1-4], have revealed several interesting properties, including discretization of electron energy levels, concentration of oscillator strength, highly polarizable excited states, increased electron-electron correlation etc. Quantum size effects have been mainly studied in II-VI semiconductors, and relatively less studied in semiconducting oxides [5].

Copper oxide is a covalent semiconductor, having a band gap of about 1.4 eV [6]. The optical properties of CuO are complicated by the strong electron correlation, which exists in this narrow band semiconductor. It would be highly interesting to study these correlation effects in reduced dimensions of the solid, where one can expect the electron correlation effects to be more pronounced. Optical techniques are the most common techniques to study the quantum size effects. Orel *et al.* [9] have reported structural studies of CuO nanoparticulate films using x-ray diffraction, scanning electron microscopy and infrared spectroscopy. Xu *et al.* [10] have reported Raman studies on CuO nanoparticles. Magnetic properties of oxide nanoparticles have attracted considerable attention [11-15]. Studies on CuO nanoparticles in the size regime, 12-50 nm [7, 8] have been reported by Palkar and Ayyub. They have synthesized a series of oxide nanoparticles [18] using chemical routes. They observed that small sized, (diameter less than 25 nm) CuO nanoparticles were not stable [7]; cubic and more ionic Cu₂O was formed, in smaller size regime. They also proposed that the ionic character of a solid tends to increase with reduction in particle size. They have, also observed an increase in ionicity, with decrease in size, in the case of other oxide nanoparticles such as Fe₂O₃ and Al₂O₃.

Here, we describe studies on CuO nanoparticles, in a much smaller size regime. A novel electrochemical method has been established, for the synthesis of CuO nanoparticles. This method is reported to yield small size distributed metallic nanoparticles [16]. Moreover, electrochemical route has viability for commercial production of nanoparticles. This fact is significant from the viewpoint of application of CuO in catalysis. Small sized, stable CuO

nanocrystals were obtained. X-ray diffraction, and infrared spectroscopic investigations, clearly shows CuO formation. Thus the present investigations quantitatively support the hypothesis proposed by Palkar *et al.* [7] but at much lower sizes. The present investigations indicate that, the stability of the nanoparticles is not only a function of size, but is also governed by the legends passivating the nanoparticles. Optical measurements reveal quantum size effects in CuO nanoparticles.

2. Experiment

Stable CuO nanocrystals, having sizes 10nm and 12nm were synthesized using an electrochemical route. Basic structural and spectroscopic characterization of the tetra-trimethyl ammonium-bromide (TTAB) capped, CuO nanoparticles have been carried out using x-ray diffraction, optical absorption spectroscopy, Fourier transform infrared spectroscopy.

CuO nanocrystals were synthesized at room temperature, by an electrochemical route, which is a modified version of the one proposed by Reetz and Helbig [16] for metal nanocrystals. A schematic diagram of the electrochemical setup used for the synthesis of cupric oxide nanocrystals in our laboratory is shown in Figure 1. The electrolytic bath consisted of acetonitrile and tetrahydrofuran (THF) mixed in the ratio 4:1, in which high purity copper and platinum foils (1cm x 1cm) served as anode and cathode respectively. The capping agent tetra-trimethyle ammonium-bromide (TTAB) also served as the electrolyte. Electrolysis was carried out in nitrogen atmosphere for a few hours in constant current mode. Current density was maintained at 10mA/cm² to obtain 10 nm and 20mA/cm² for 12nm sized CuO particles. The molarity of TTAB in the chemical bath was varied from 0.1 mM to 0.9 mM. Marginal change in the average size of the nanocrystals, with TTAB molarity is observed. The black CuO nanocrystals remain suspended in the solvent and are separated out by centrifugation. On drying, a free flowing powder of CuO nanocrystals is obtained. Formation of CuO nanoparticles is different from that of bulk CuO.

Nanocrystal size estimated by XRD indicates that the amount of the current density water in the electrochemical bath decides the size of the nanocrystals. It may be noted here that, in case of metallic nanoparticles [16], size was controlled by varying the current density.

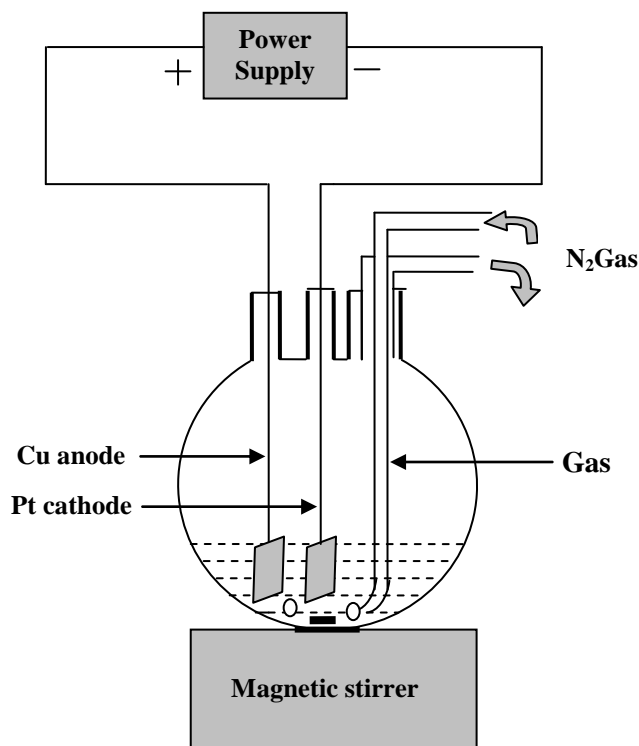


Fig. 1: Electrochemical cell for synthesis of CuO nanoparticles.

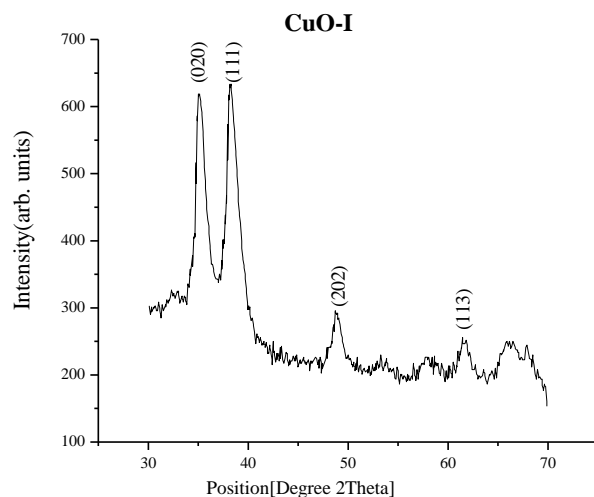
The mechanism of cluster formation can be explained as follows. On anodic dissolution, liberated Cu ions form nanoclusters which get oxidized immediately after formation and subsequently get passivated by active TTAB species. The mechanism of capping can be tentatively explained as follows. Due to adsorbed oxygen, the surface of CuO clusters is negatively charged. Tetra-trimethyl ammonium-bromide $\{[\text{CH}_3(\text{CH}_2)_7]_4\text{NBr}\}$ in solution gives R_4N^+ and Br^- ions. These R_4N^+ ions thus electrostatically bind to the negatively charged CuO surface thereby preventing agglomeration. The possible reason for oxidation of Cu is due to residual oxygen in the cell. Chemical analysis of the CuO nanoparticles indicates presence of nitrogen (due to TTAB). Presence of capping agent TTAB on the surface of CuO nanoparticles is also revealed from infrared absorption spectroscopy.

X-ray diffraction was carried out on a PHILIPS X Petr PRO powder X-ray diffractometer, using Cu K_α ($\lambda = 1.54178 \text{ \AA}$) as the incident radiation. Size of the nanocrystals were determined from x-ray line broadening, using the Scherrer formula ($D = 0.9\lambda/\beta\cos\theta$), where D is the particle diameter, λ is the wavelength of the incident x-ray, β is the full width at half maximum of the diffraction peak and θ is the Bragg angle. Optical spectrophotometric measurements were carried out on a SHIMADZU UV-VIS (UV-1650PC) double beam spectrophotometer. Fourier transform infrared (FTIR) spectra of the quantum dots were taken at room temperature, using a FTIR-H400/89, SHIMADZU series FTIR spectrophotometer. The samples were embedded in the host media nujol, and scanned from 4000 cm^{-1} to 400 cm^{-1} .

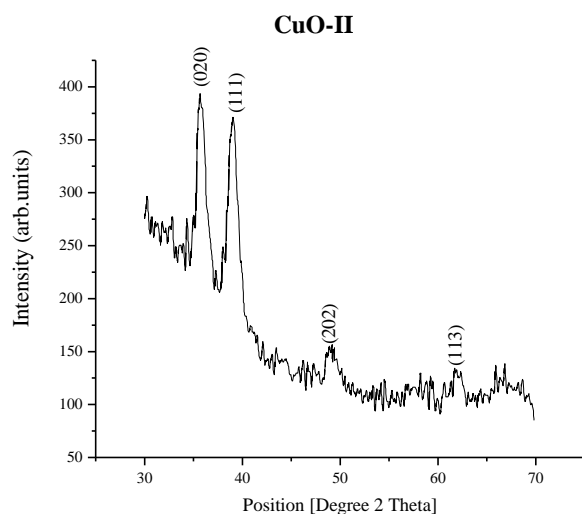
3. Results and Discussion

3.1 X-ray Diffraction Studies

Figure 2: shows the x-ray diffraction patterns of CuO nanocrystals of two different average diameters. Average nanocrystal diameters as estimated from XRD using the Scherrer formula were about 10 nm and 12 nm for two different sized clusters, henceforth referred to as CuO-I, CuO-II respectively. Inter-planar distances obtained from XRD patterns match well with standard diffraction data (JCPD card no. 5-0661), confirming a monoclinic crystal structure. Although no change in lattice constants were observed for CuO-II and CuO-III nanocrystals, CuO-I showed about 1% lattice contraction, compared to bulk CuO. Lattice contraction has been observed in several nanocrystalline systems [17, 18]. Increase in surface stress is assumed to be one of the key factors in lattice contraction. Mainly, XRD was carried out to confirm the parity of nanocrystal. XRD spectra shows only CuO phase. The number of atom in 10nm (diameter) particle size is approximately 6371. XRD patterns of CuO nanoparticles scanning from 30° - 70° generating the lines (020), (111), (202), (113) at 34° , 38° , 48° , and 62° in CuO-I sample and at 35° , 38° , 48° , and 62.5° in CuO-II sample respectively.



XRD pattern of sample A



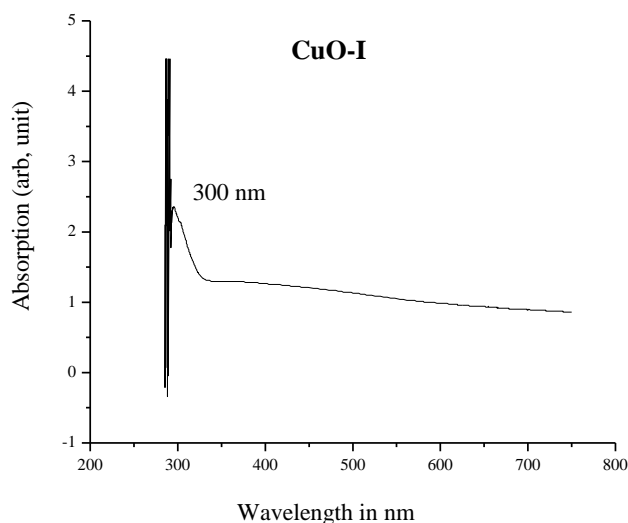
XRD pattern of sample B

Fig. 2: X-ray diffraction patterns of CuO nanocrystals exhibiting monoclinic phase. Average diameter determined using Scherrer formula for (a) CuO-I (b) CuO-II nanocrystals were 10 nm and 12 nm respectively

3.2 Optical Absorption Spectroscopy

Apart from Raman and infrared absorption studies, reports on optical properties of CuO especially in the ultra violet to visible region are very limited. A wide variety of features have been observed in the CuO optical absorption spectrum, probably dependent on the history of the sample. Good quality single crystals have not been studied in detail using optical spectroscopes except by Marabelli *et al.* [19].

Figure 3: shows the optical absorption spectra of CuO nanoparticles, dispersed in acetonitrile. Slight shift in the optical absorption feature towards higher energy, can be seen with reduction in cluster size. For CuO-II, the optical absorption feature is seen at about 286 nm (4.34 eV), whereas in the case of CuO-I, this feature is visible at about 300 nm (4.13 eV). The optical absorption spectra of CuO nanocrystals show very broad features. Marabelli *et al.* [19] have studied the optical absorption edge of CuO single crystals by reflectance and transmittance measurements at different temperatures.



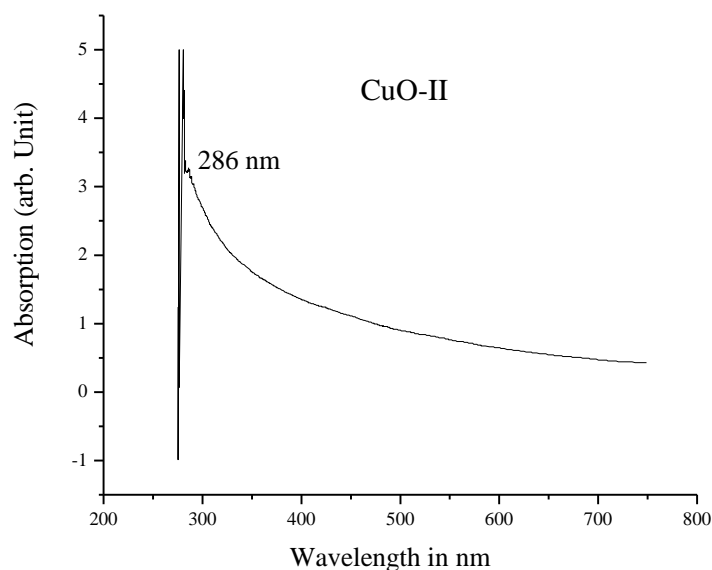


Fig. 3: Optical absorption spectra of (a) CuO-I (10nm) and (b) CuO-II(12nm) nanocrystals dispersed in acetonitrile, showing absorption feature at 300 nm and 286 nm respectively.

The tailing in optical absorption spectra has been predicted to be due to strong electron phonon coupling and presence of narrow hybridized *d* levels in the forbidden gap region. Wieder and Czanderna [20] have studied the transmittance and reflectance of CuO films in the region 400-800 nm. For 88 nm thick CuO film, the transmittance was found to decrease gradually from 800 to 400 nm. No peak was observed in this region. Koffyberg and Benko [21] have carried out studies on lithium doped cupric oxide. They have reported an indirect allowed band gap of 1.35 ± 0.02 eV, and a direct allowed interband transition at 3.25 ± 0.05 eV for CuO. Recently, Ito *et al.* [22] have measured the real and imaginary parts of the dielectric function of polycrystalline CuO, using spectroscopic ellipsometry. They observed four distinct absorption features at energies 1.6 eV, 2.0 eV, 2.6 eV and 3.4 eV. The feature located at 3.4 eV was the most prominent. The transition at 1.6 eV was attributed to band-to-band transition, while other transitions were not analyzed. The optical absorption spectra of CuO quantum dots in the present investigations reveal features at 4.13 eV and 4.34 eV for CuO-I, CuO-II nanocrystals respectively. This is probably the same feature observed by Ito *et al.* [22] and Koffyberg and Benko [21] at about 3.25 eV, albeit blue shifted due to quantum size effects. The indirect allowed transition located at 1.35 eV is not visible in the present study on CuO nanoparticles. The gradual increase of the optical absorption over a wide spectral range, along with the indirect nature of the transition and the size distribution of the nanoparticles could be responsible for this. The enhanced spatial overlap between the electron and hole wave functions leads to an increase in oscillator strength with decreasing particle size. This fact is well revealed in Figure 3.

It would be interesting to examine quantum size effects in CuO nanocrystals in detail. However, the validity of simple treatment viz. effective mass approximation in case of CuO is questionable. Band structure calculations and optical studies on CuO are limited [23-27] even in its bulk form. Using the values of effective masses of electron and hole reported by Ching *et al.* [23], Koffyberg and Benko [21] and Warren *et al.* [28], the Bohr exciton radius is found to lie between 6.6 nm and 28.72 nm. In either case, CuO nanoparticles studied in the present case (radius ranging between 6 nm and 5nm) are well within the strong confinement regime. This can also be seen from the optical absorption spectra which show a shift towards higher energy with decrease in size of the nanocrystals.

3.3 Infrared Absorption Studies

Group theoretical calculations and experiments, [29-34] suggest that the six IR bands of CuO are located at about 147 (B_u), 161 (A_u), 321 (A_u), 478 (A_u), 530 (B_u) and 590 (B_u) cm^{-1} . Reported values by different authors vary slightly, due to variation in sample type, temperature and also due to broadness of the spectrum.

Figure 4: exhibits the FTIR transmission spectra of CuO-I and CuO-II quantum dots, at room temperature. For CuO-I quantum dots, three main vibrational modes are observed at 468 (A_u), 529 (B_u), and 590 (B_u) cm^{-1} . In the case of CuO-II quantum dots, the broad peaks are centered at about 454 (A_u), 526 (B_u) and 587 (B_u) cm^{-1} . The weak feature that can be seen at about 540 cm^{-1} in both spectra, is due to the capping agent TTAB. The high frequency mode at about 590 cm^{-1} is reported [30] to be a Cu—O stretching along the [101] direction and the mode at about 530 cm^{-1} is reported to be due to Cu—O stretching along [101]. Moreover, no mode due to Cu_2O is seen (infrared active modes of Cu_2O , appear at 610 cm^{-1} and 147 cm^{-1}) [35]. This goes to prove that the quantum dots comprise of purely CuO phase, without any trace of Cu_2O being present.

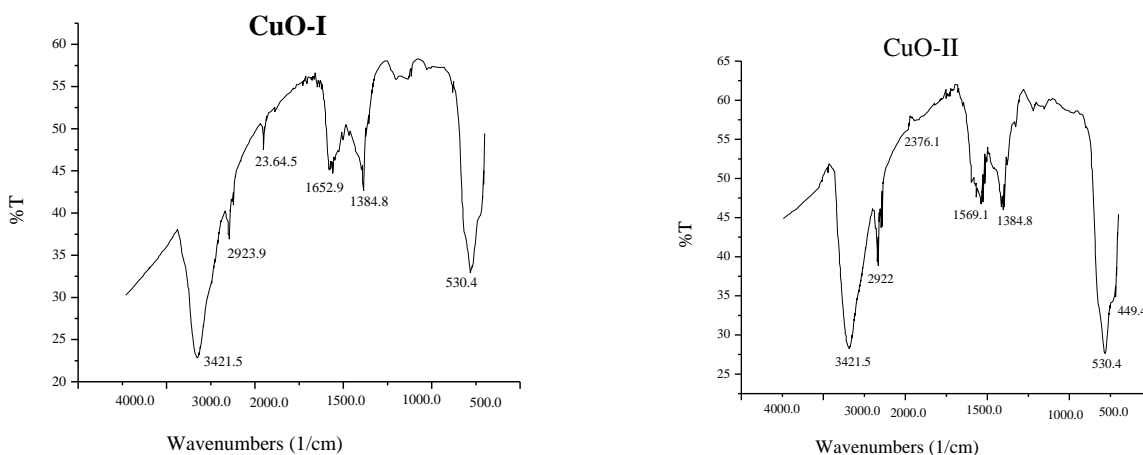


Fig. 4: Fourier transform infrared spectra of CuO-I and CuO-II nanocrystals. CuO-I sample shows 530.4, 1384.8, 1652.9, 2364.6, 3421.5 vibrational mode while CuO-II sample shows 449.4, 530.4, 1384.8, 1569.9, 2376.1, 2922, 3421.5 respectively.

Conclusion

In summary, stable single phase quantum dots of cupric oxide, having low size distribution were synthesized at room temperature, using a novel and simple electrochemical synthesis route. This method gives a high yield of sample, without any undesired side products, allowing easy isolation of the quantum dots from the solution. Cupric oxide quantum dots of two different sizes were synthesized. The crystal structure of CuO nanoparticles is the same as that of bulk CuO, though some amount of lattice contraction could be seen for quantum dots in the size regime of 10nm and 12nm.

References

- [1] A. D. Yoffe, *Adv. Phys.* **42**, 173 (1993).
- [2] Y. Kayanuma, *Phys. Rev. B* **38**, 9797, (1988).
- [3] L. E. Brus, *IEEE J. Quantum Electron.* **22**, 1909 (1986).
- [4] M. V. Rama Krishna and R. A. Friesner, *Phys. Rev. Lett.* **67**, 629 (1991).
- [5] S. Mahamuni, K. Borgohain, B. S. Bendre, V. J. Leppert, and S. H. Risbud, *J. Appl. Phys.* **85**, 2861 (1999).

- [6] J. Ghijsen, L. H. Tjeng, J. van Elp, H. Eskes, J. Westerink, G. A. Sawatzky, and M. T. Czyzyk, *Phys. Rev. B* **38**, 11322 (1988).
- [7] V. R. Palkar, P. Ayyub, S. Chattopadhyay and M. Multani, *Phys. Rev. B* **53**, 2167 (1996).
- [8] P. Ayyub, V. R. Palkar, S. Chattopadhyay, and M. S. Multani, *Phys. Rev. B* **51**, 6135 (1995).
- [9] B. Orel, F. Svegli, N. Bukovek and M. Kosec, *J. Non-Crystalline Solids* **159**, 49 (1993).
- [10] J. F. Xu, W. Ji, Z. X. Shen, W. S. Li, S. H. Tang, X. R. Ye, D. Z. Jia and X. Q. Xin, *J. Raman Spectroscopy* **30**, 413 (1999).
- [11] T. I. Arbutova, I. B. Smolyak, A. A. Samokhvalov and S. V. Naumov, *Journal of Experimental and Theoretical Physics* **86**, 559 (1998).
- [12] T. I. Arbutova, S. V. Naumov, A. A. Samokhvalov, B. A. Gizhevski, V. L. Arbutov and K. V. Shalnov, *Physics of Solid State* **43**, 878 (2001).
- [13] G. Boschloo and A. Hagfeldt, *J. Phys. Chem. B* **105**, 3039 (2001).
- [14] A. Punnoose, M. Magnone, M. S. Seehra and J. Bonevich, *Phys. Rev. B* **64**, 174420 (2001).
- [15] M. S. Seehra and A. Punnoose, *Phys. Rev. B* **64**, 132410 (2001).
- [16] M. T. Reetz and W. Helbig, *J. Am. Chem. Soc.* **116**, 7401 (1996).
- [17] H. Wasserman and J. Vermaak, *Surf Sci.* **22**, 164 (1970).
- [18] H. Wasserman, J. Vermaak, *Surf Sci.* **32**, 168 (1972).
- [19] F. Marabelli, G. B. Parravicini, and F. Salghetti-Drioli, *Phys. Rev. B* **52**, 1433 (1995).
- [20] H. Wieder and A. W. Czanderna, *J. Appl. Phys.* **37**, 184 (1966).
- [21] F. P. Koffyberg and F. A. Benko, *J. Appl. Phys.* **53**, 1173 (1982).
- [22] T. Ito, H. Yamaguchi, T. Masumi and S. Adachi, *J. Phys. Soc. Jpn.* **67**, 3304 (1998).
- [23] W. Y. Ching, Y. N. Xu and K. W. Wong, *Phys. Rev. B* **40**, 7684 (1989).
- [24] M. Takahashi and J. Igarashi, *Phys. Rev. B* **56**, 12818 (1997).
- [25] J. Laegsgaard and A. Svane, *Phys. Rev. B* **55**, 4138 (1997).
- [26] H. Eskes, L. H. Tjeng and G. A. Sawatzky, *Phys. Rev. B* **41**, 288 (1990).
- [27] M. Grioni, M. T. Czyzyk, F. M. F. de Groot, J. C. Fuggle and B. E. Watts, *Phys. Rev. B* **39**, 4886 (1989).
- [28] S. Warren, W. R. Flavell, A. G. Thomas, J. Hollingworth, P. L. Wincott, A. F. Prime, S. Downes and C. J. Chen, *Phys.: Condens. Matter* **11**, 5021 (1999).
- [29] S. Guha, D. Peebles, and T. J. Wieting, *Phys. Rev. B* **43**, 13092 (1991).
- [30] G. Kliche, and Z. V. Popovic, *Phys. Rev. B* **42**, 10060 (1990).
- [31] H. Hagemann, H. Bill, W. Sadowski, E. Walker, and M. Francois, *Solid State Commun.* **73**, 447 (1990).
- [32] Z. V. Popovic, C. Thomsen, M. Cardona, R. Liu, G. Stanisc, R. Kremer and W. Konig, *Solid State Commun.* **66**, 965 (1988).
- [33] L. Degiorgi, E. Kaldis, and P. Wachter, *Physica C* **153**, 657 (1988).
- [34] S. N. Narang, V. B. Kartha, and N. D. Patel, *Physica C* **204**, 8 (1992).
- [35] E. C. Heltemes, *Phys. Rev.* **141**, 803 (1966).